*First Deliverable to*

# The FERMI @ Elettra
# Technical Optimization Study

*entitled:*

## "Preliminary Parameter Set and Initial Studies"

*submitted by:*

**Lawrence Berkeley National Laboratory**
**1 Cyclotron Road**
**Berkeley, CA 94720**

**John Byrd**
**John Corlett**
**Larry Doolittle**
**William Fawley**
**Steven Lidia**
**Gregory Penn**
**Alex Ratti**
**John Staples**
**Russell Wilcox**
**Jonathan Wurtele**
**Alexander Zholents**

**August 1, 2005**

**This report constitutes the first deliverable of LBNL's contracted role in the FERMI @ Elettra Technical Optimization study. It describes initial studies of design, layout, and parameters for the proposed facility.**

# Background summary of the Technical Optimization Study

The goal of the FERMI @ Elettra Technical Optimization Study is to produce a machine design and layout consistent with user needs for radiation in the approximate ranges 100 nm to 40 nm, and 40 nm to 10 nm, using seeded FEL's. The Study will involve collaboration between Italian and US physicists and engineers, and will form the basis for the engineering design and the cost estimation.

In order to achieve this goal, the study will produce physics models of the machine:

- A physics model of the electron beam
- A physics model of FEL output

The Physics Design Study will provide the conceptual layout, the parameters, and the performance specification for the FERMI @ Elettra Project, and will be accomplished in three distinct stages:

1. A "skeleton design" that provides a general layout and configuration, with a first pass at accelerator physics issues sufficient to estimate the major FEL output parameters.
2. A "conceptual design" that provides detailed accelerator physics studies of all known effects, into a self-consistent start-to-end model. FEL output will be modeled based on input from the start-to-end simulations. Physics designs will be sufficiently mature to allow engineering considerations to begin.
3. A "technical design", with a completed physics model, and including engineering concepts sufficient to allow detailed engineering to begin.

Constraints to the study parameters include:

- To use identified and existing hardware where possible
- To remain within limitations of real estate
- Construction, commissioning, and operations of the proposed machine should have minimal impact on Elettra operations and users
- To consider options allowing for future upgrades and where possible produce designs that do not to preclude future installation of interesting concepts

# Baseline Concept – Initial Layout and Parameters

**Summary of initial layout and parameters studies**

We have examined FEL sources from 10-100 nm, suitable for long pulse as well as attosecond radiation sources. The electron beam quality is crucial, and probably energy spread is more important than transverse emittance. Analytical tools are yielding insights and corroborate simulation results. Preliminary simulations suggest 100's MW to 1 GW output powers from a 1 GeV electron beam, using seeded harmonic cascade FEL's. Areas highlighted for further study are:

- Beam dynamics, especially longitudinal phase space
- RF cavities must be carefully characterized, and wakefields in the linac will have a strong impact on performance
- Minimize phase space distortions during acceleration and compression
- Start-to-end simulations will be essential
- Sensitivity studies
- We anticipate using alternative design for modulators
- Other modes of operation and FEL designs will be considered
- Input from potential users will be very important

**Overview of the layout**

The FERMI @ Elettra project will make use of the existing ~ 1 GeV linac to provide high-quality electron beams to seeded FEL's to be built on a site adjacent to the Elettra storage ring. A preliminary sketch of the layout is shown in Figure 1. It will be important to maximize space for FEL and experimental halls, with preliminary footprint areas of approximately:

- ~40x20 m undulator hall, to accommodate several FEL's
- ~30-40 m beamline length

Figure 2 shows as preliminary sketch of a proposed configuration of the major linac components, and indicates the linac tunnel extension (backwards), two bunch compressors, and inclusion of CERN accelerating structures as well as existing accelerating sections.
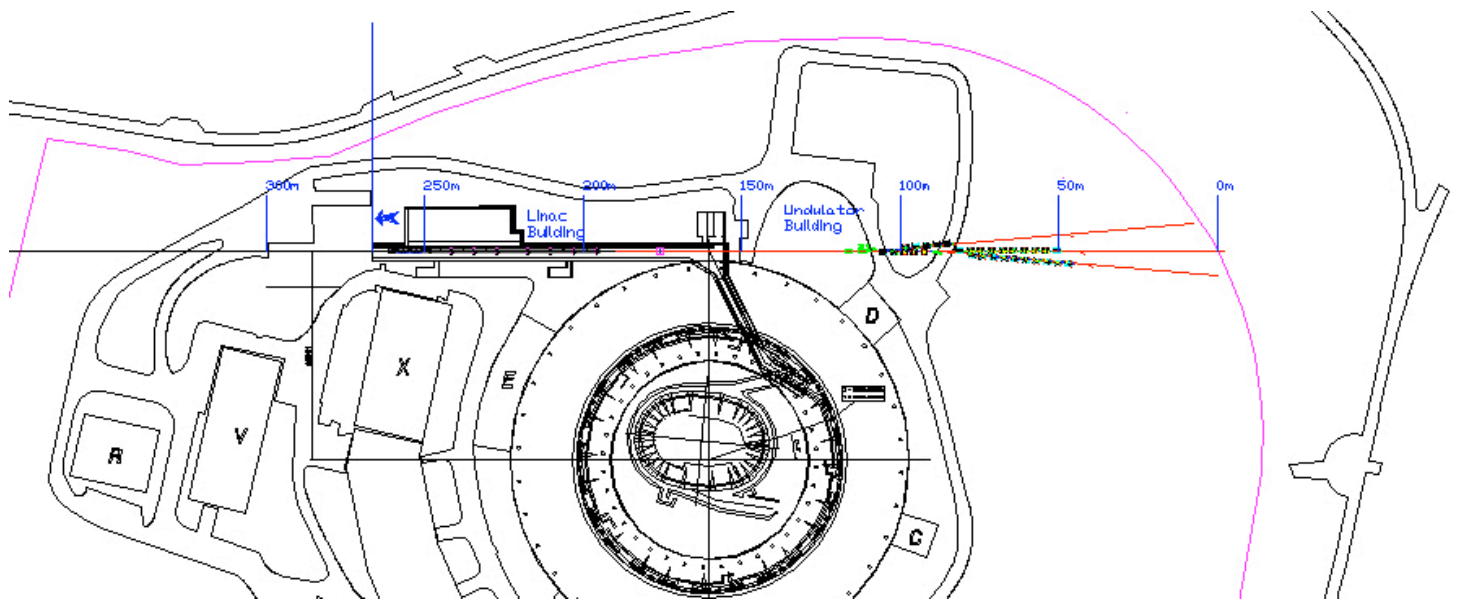
Figure 1 – Sketch of the overall layout of the linac, transport line, FEL's and beamlines at the Sincrotrone Trieste site
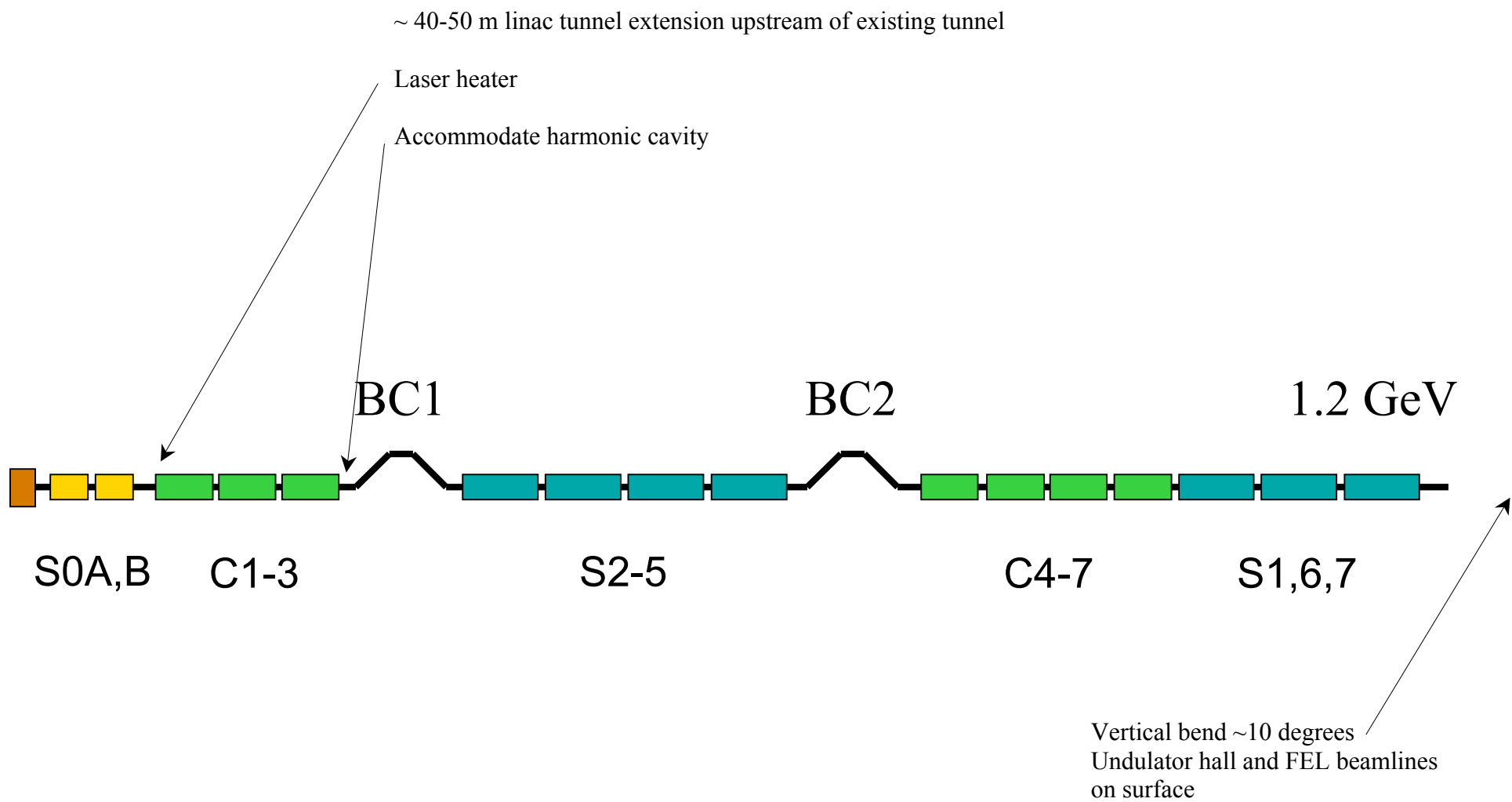
~ 40-50 m linac tunnel extension upstream of existing tunnel

Laser heater

Accommodate harmonic cavity

BC1

BC2

1.2 GeV

S0A,B

C1-3

S2-5

C4-7

S1,6,7

Vertical bend ~10 degrees
Undulator hall and FEL beamlines
on surface

Figure 2 – Sketch of the main linac components.

High-level parameters for the configuration sketched in Figure 2 are:

| | |
|---|---|
| FEL-I output wavelength | ~80 nm to ~30 nm |
| FEL-II output wavelength | ~35 nm to ~7 nm |
| Electron beam energy | 1.2 GeV |
| Peak current | >400 A |
| Uncorrelated energy spread $\sigma_E$ (rms) | 150 keV |
| Emittance (slice) | < 2 mm-mrad |
| Bunch length at FEL | ~ 1 ps |
| Bunch length at gun | ~ 5 ps |

The FEL output's should overlap to ensure continuous coverage of the spectrum, with a goal of extending each FEL's output to shorter wavelength:

| | |
|---|---|
| FEL-I output wavelength | <40 nm |
| FEL-II output wavelength | <10 nm (~7 nm) |

A single FEL would be operational at a time, with a "DC" magnetic transport selecting one or other FEL to be fed from the linac. Pulse duration would initially be of order picoseconds, with options for narrow bandwidth (long pulse) and options for ultrafast production (very short pulse).

The group at LBNL has considered the FERMI design requirements and performance based on early studies and guidelines communicated to us. We have considered the given design parameters as preliminary guidelines, and make the following observations and comments for a seeded harmonic cascade FEL facility:

- favor high beam energy (1 GeV or greater)
- favor low energy spread (< 200 keV $\sigma_E$)
- consider 1 and 2 stages of harmonic generation
- in contrast to high-gain SASE, keep to low-gain regime
    - yields timing control, low bandwidth, consistency
    - relies on strong bunching, made possible by low energy spread $\sigma_E$
- synchronized FEL output
- tunable FEL output
- 50 Hz rep rate
- ranging from ~100's fs coherent light to sub-femtosecond pulse

We have considered variable bunch compression, and expect current, energy spread, 1/(usable bunch length) to all scale linearly with each other.

**Injector systems initial layout and parameters**

Injector systems consist of:
- Drive laser
- RF gun
- Booster linacs
- Harmonic cavities

Injector systems primary design parameters are:
- Energy
- Energy spread
- Charge
- Bunch length
- Slice and projected emittances
  - To be evaluated
    - At gun exit
    - At entrance to bunch compressor (BC1) or main linac

Injector tuning requires optimization of laser profiles and timing, RF amplitudes and phases, emittance compensation schemes, harmonic cavity amplitude and phase. Initial electron bunch parameters for the long bunch case with low current/charge density at cathode are:

| | |
|---|---|
| Charge | 0.5 nC |
| Pulse duration at gun exit | 10-15 ps |

and for the short-bunch case:

| | |
|---|---|
| Charge | 0.3 nC |
| Pulse duration at gun exit | 5 ps |

Bunch compression schemes using 'standard' magnetic chicane compression and novel velocity compression have been considered. A preliminary investigation of using a magnetic chicane with a long bunch of 10-15 ps FWHM, 0.5-1.0 nC suggest this is a good choice in delivering high brightness beams.

Velocity compression uses booster cavities near zero-crossing, and simplifies the layout requiring no chicanes. Emittance compensation, however, is more difficult due to nonlinear, correlated energy spread, and the technique requires a more complicated tuning scheme for linacs and solenoids. It is estimated that the technique can achieve ~0.5 kA, but needs additional harmonic cavities. Initial studies suggest it may be difficult to achieve $2\pi$ mm-mrad (projected), and the uncorrelated energy spread needs to be evaluated.

Figure 3 shows ASTRA simulation results for a BNL/SLAC/UCLA RF gun, followed by existing buncher cavities S0A and S0B, and an S1 accelerating section. Parameters at the cathode are 0.5mm rms laser spot, 0.60 mm-mrad rms emittance, 15 ps flattop, 2 ps rise/fall, 0.5 nC charge.

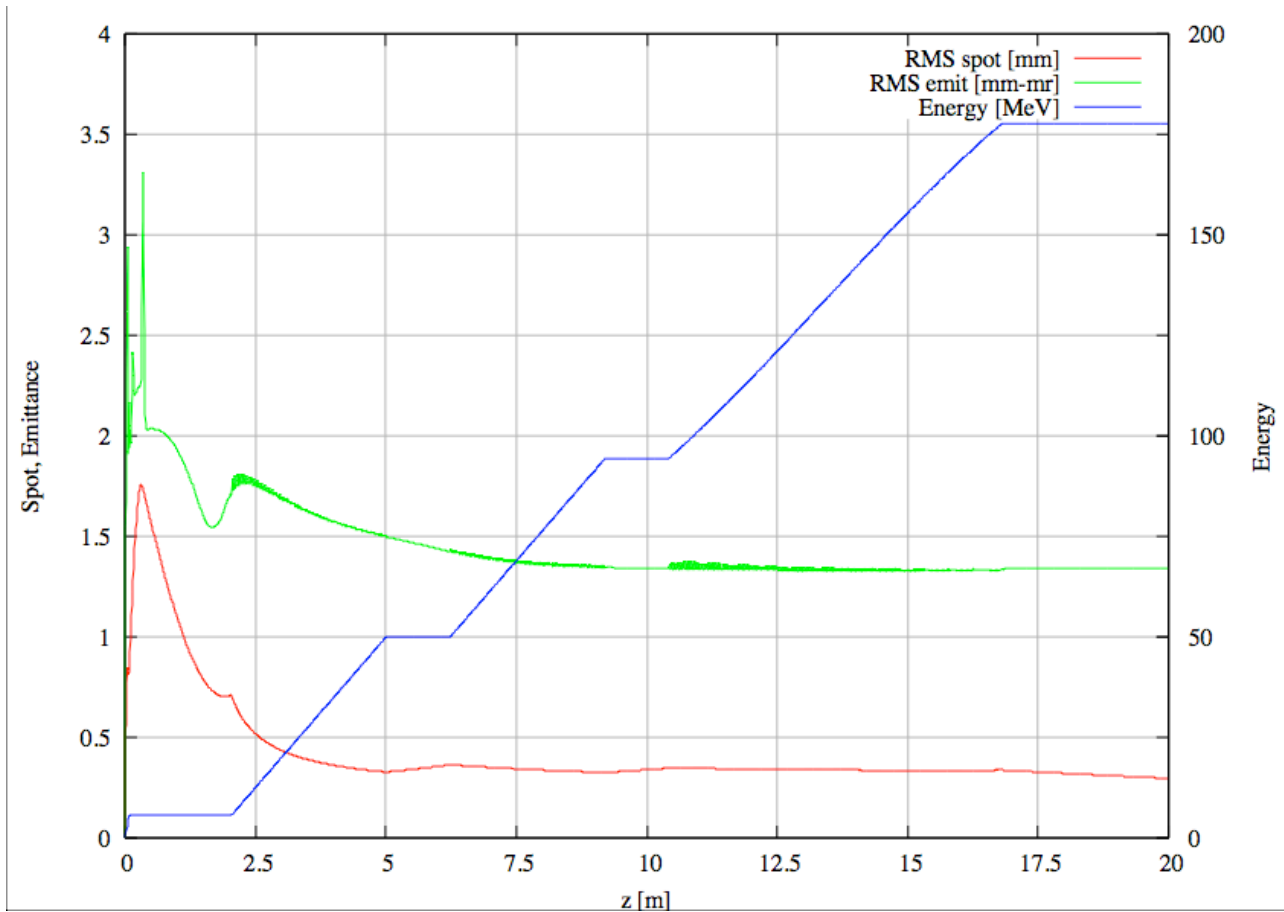Table 1 summarizes electron beam parameters at various points along the accelerator.

Figure 3 - ASTRA simulation results for an injector without bunch compressor.
Parameters are given in the text above.

Table 1 – Initial estimates of electron beam parameters at various points along the accelerator

| | Gun Exit | BC1 Entrance | FEL Entrance |
|---|---|---|---|
| Energy (maximum realizable value) (MeV) | ~5-6 | 263 | 1435 |
| Energy Spread | ~10 keV | ~10 keV 1% corr. | 150 keV ? |
| Q (pC) | ~500 | ~500 | ~500 |
| Bunch Length (ps) (FWHM) | 5-7 | 5-7 | 1 |
| Emittance (mm mrad) (projected) | <3 (<2 in simulations) | <3 (<2 in simulations) | <3 |

**Choice of RF gun**

The difference between 'European' S-band and 'U.S.' S-band frequencies makes it difficult to take an established gun design and apply it to the FERMI @ Elettra project. Some re-design or adaptation will be needed, adding cost to project resources and schedule and also affecting the physics design. Possible designs include the BNL/SLAC/UCLA/AES designs (I), and the LCLS gun design (II) which has received intensive physics and engineering to achieve performance goals but has not yet been built. 50Hz rep rate may be challenging for gun I, gun II is designed to operate at 120Hz. It may be appropriate to plan for an initial rf gun to demonstrate FEL, with a future upgrade (new gun) following in 1-2 years.

**Choice of photocathode laser**

The choice of laser is strongly coupled to the choice of photocathode material. Need ~4eV photons, QE (Cu) ~several $10^{-5}$. We note that some interesting work at ~6 eV has recently been performed at UCSC Brescia, with QE (Cu) ~$10^{-4}$. There appears to be no compelling reason to adopt Mg over Cu photocathodes, experience at the SLAC GTF suggests worse dark current with Mg, probably due to breakdown around cathode plug rf joint. Laser pulse shaping and amplitude control is essential for high-quality electron bunch production. Temporal shaping may be achieved with AOPDF, SLM, etc, spatial profiling with deformable mirrors, refractive beam shapers, SLM. Pulse shape requirements and techniques need top be considered in the initial design of the drive laser system. For example, Figure 4 shows a photocathode system designed at LBNL and includes spatial and temporal shaping with a (modified) commercial laser.

Initial photocathode laser systems requirements are
- 5-10 ps flattop
- 0.5-1 ps rise/fall
- Laser pulse energy ~100 µJ (including overhead for shaping, and losses) to provide ~0.5 nC, with cathode QE ~$2-3\times10^{-5}$

**Vertical ramp from linac tunnel to undulator hall**

Significant space may be saved by increasing the inclination of the vertical ramp from the underground linac tunnel to the undulator hall on the surface. Figure 5 sketches the geometry, for two angles of 30° and 5° over a vertical height of approximately 5 m. A bunch compressor may be included in the inclined transport line, which fits in ~8 m of longitudinal space. We note that a similar design can be used for an extraction lattice leading to FEL-I.
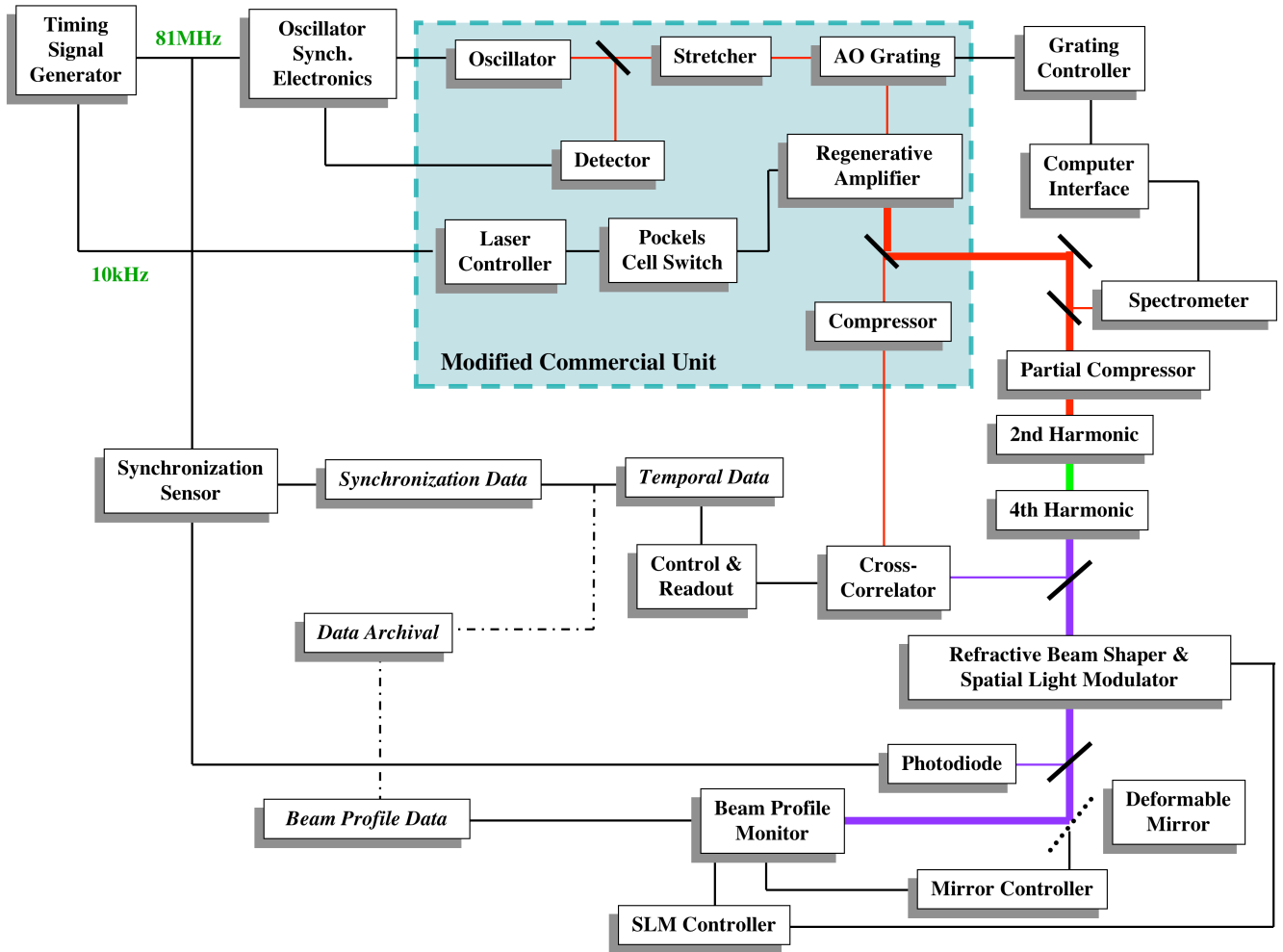
Figure 4 - Photocathode system designed at LBNL with a (modified) commercial laser and spatial and temporal pulse shaping
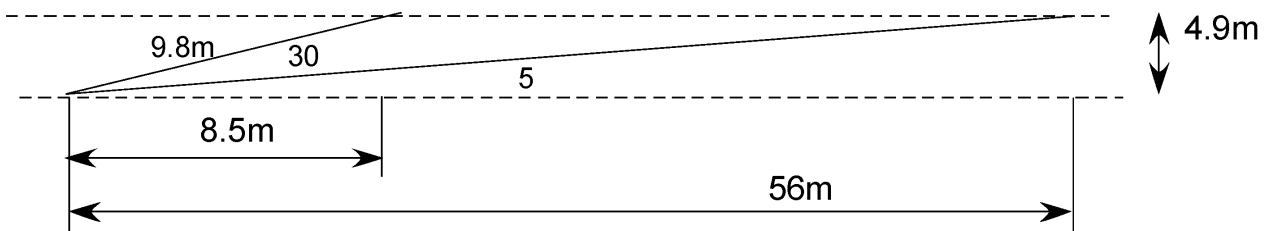


Figure 5 – Geometry of the vertical ramp from linac centerline 4.9 m below the undulator centerline.

**Vertical ramp detailed studies**

Detailed analysis has been made for a 12.5º vertical ramp angle (other angles were also considered and will be discussed later). Figures 6 and 7 show plots of the Twiss functions for two variants of the vertical ramp. Both lattices have identical parts at the beginning and at the end and differ in the central part spanning between the second and the third bending magnets. We call the first lattice as the high-beta lattice and the second lattice as the low-beta lattice. All bending magnets are identical rectangular magnets and all quadrupoles are identical too. While the length of the bending magnet is somewhat constrained by CSR effects, the choice of the quadrupole magnet can be reconsidered if necessary.

The lattice is designed such as the first two bending magnets and the last two bending magnets are separated by $-I$ transport matrixes in both $x$ and $y$ planes, *i.e* $\pi$ betatron phase advance. A FODO lattice consisting of two doublets is used for this purpose. This serves the purpose of constraining the dispersion function between pairs of magnets and mitigation of the emittance excitation due to CSR effects. The lattice in the middle section is also a FODO lattice spanning over $\pi$ phase advance in both planes in the high-beta case and $3\pi$ phase advance in the low-beta case. The $-I$ transport matrix in the middle section is important for a compensation of the emittance excitation due to CSR effects. We demonstrate it by comparing the emittance excitation occurred in this lattice shown in Figure 8 with the emittance excitation in the similar lattice with $I$ transport matrix in the middle section shown in Figure 9. These plots were produced using the Elegant code with the following electron beam parameters:

| | |
|---|---|
| Energy | 1.2 GeV |
| Normalized emittance (Gaussian distribution) | 2 mm-mrad |
| Energy spread (hard edge distribution) | $1.5 \times 10^{-4}$ |
| Bunch length (hard edge distribution) | $1.5 \times 10^{-4}$ m |
| Charge | 0.5 nC |
| Number of macro particles in simulation | 106 |

In principle, the electron beam optics in $y$ plane is not constrained by considerations of the emittance excitation and can be made differently, but we find convenient and rather attractive to use a simple FODO lattice with equal focusing strengths between focusing and defocusing quadrupoles.

Figure 10 shows the electron beam energy distribution (left histogram), peak current (right histogram) and longitudinal phase space (central plot) at the end of the vertical ramp for a lattice with $-I$ transport matrixes in the middle section. It is seen here that the CSR effects are only visible at the edges of the electron bunch. We also studied few more ramp angles and explored what would happen if the electron bunch charge were raised to 2 nC leading to 2 kA peak current. These results are summarized in Table 2 where we show a fractional increase of the electron beam emittance.
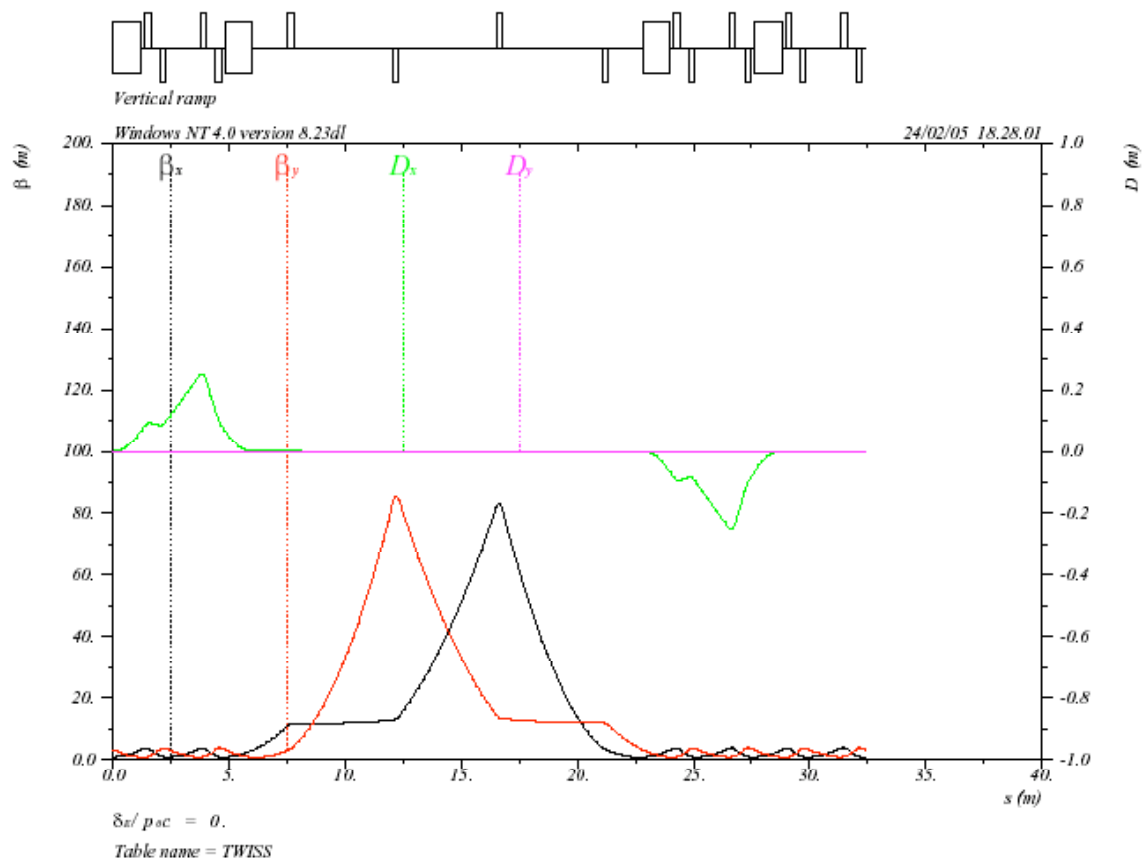
Figure 6 – The high-beta lattice of the vertical ramp with angle 12.5°

Table 2 - The fractional increase of the electron beam emittance at the end of the vertical ramp: $\varepsilon_{out}/\varepsilon_{in}$

| Ramp angle | $\varepsilon_{out}/\varepsilon_{in}$ (for 0.5 nC) | $\varepsilon_{out}/\varepsilon_{in}$ (for 2 nC) |
|------------|------------------|------------------|
| 10° | 1.005 | 1.11 |
| 12.5° | 1.01 | 1.33 |
| 15° | 1.02 | 1.80 |

We also obtained $\varepsilon_{out}/\varepsilon_{in} = 1.054$ for 1 nC and for a 12.5° ramp angle.
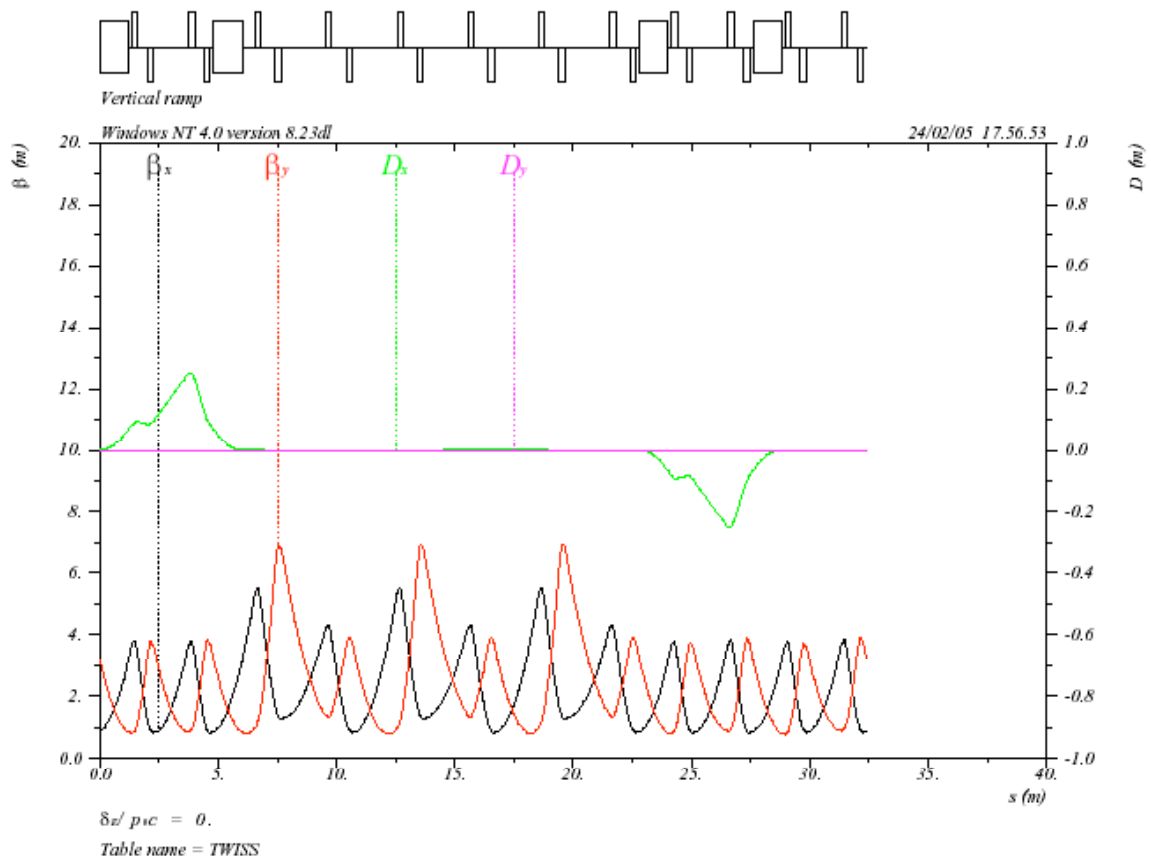
Figure 7 – The low-beta lattice of the vertical ramp with angle 12.5°
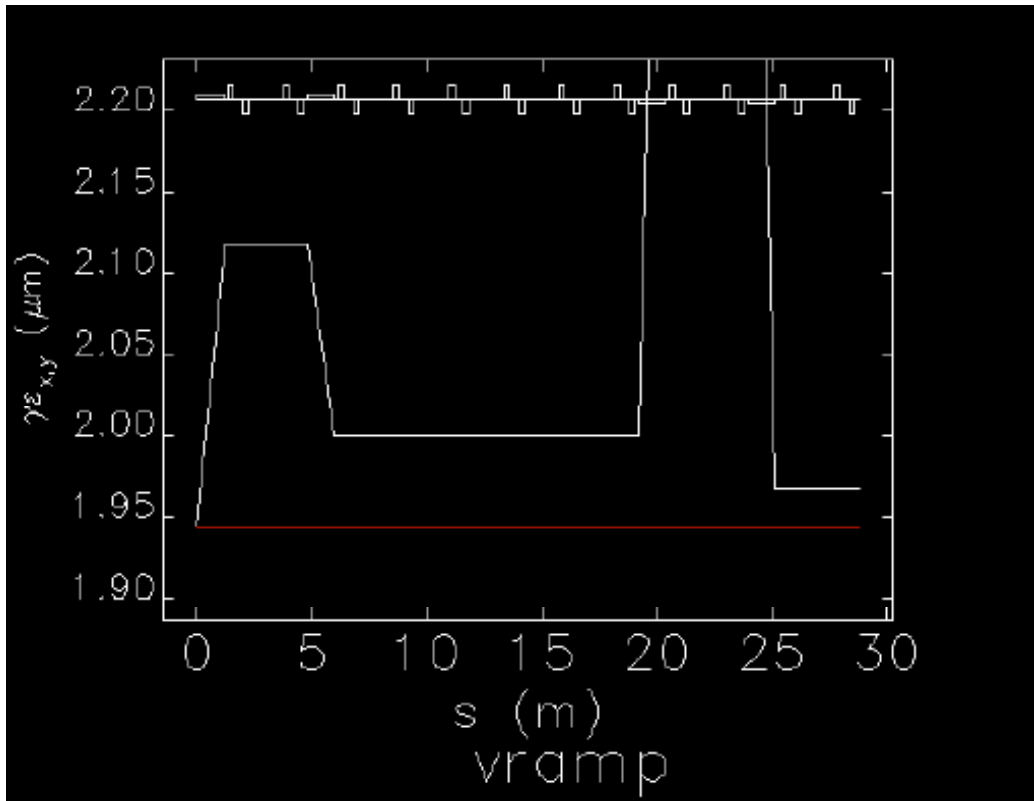
Figure 8 - Normalized electron beam emittance (white line) along the lattice for a case of –*I* transport matrix in the middle section.
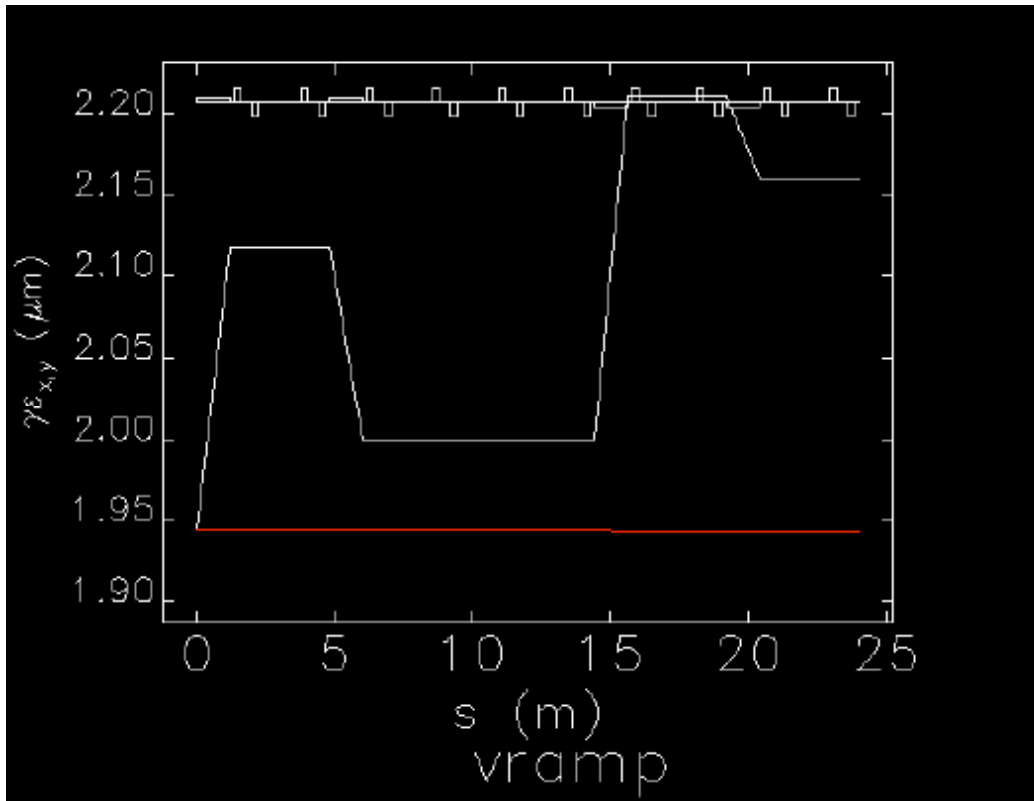
Figure 9 - Normalized electron beam emittance (white line) along the lattice for a case of *I* transport matrix in the middle section.
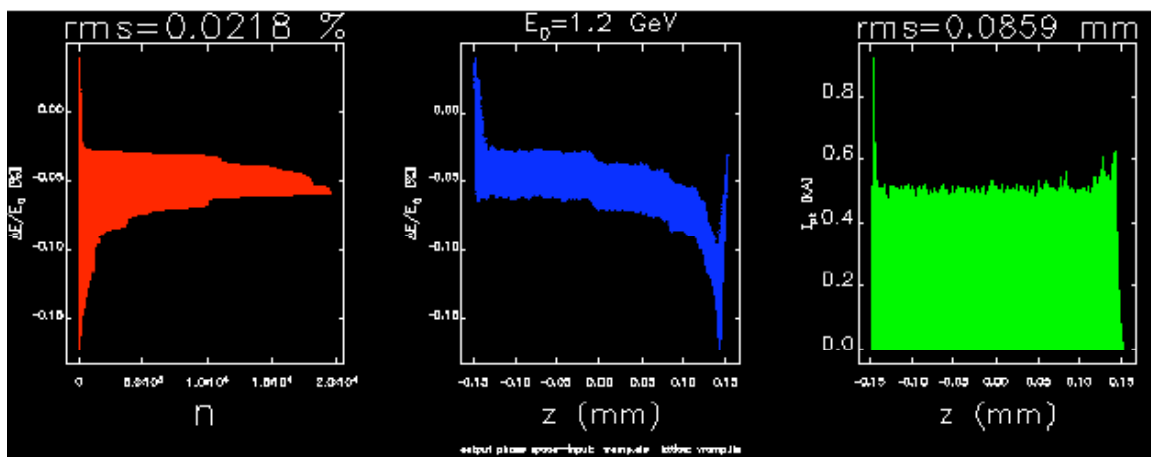


Figure 10 - The electron beam energy distribution (left histogram), peak current (right histogram) and longitudinal phase space (central plot) at the end of the vertical ramp for a lattice with –*I* transport matrixes in the middle section.

Figure 11 shows the electron beam trajectory for the lattice with the 12.5° ramp angle. It is seen there that the vertical ramp requires a tunnel with approximate length of 29 m.

The R56 matrix coefficient for a lattice with the 12.5° ramp angle is -0.0096 m and T566 matrix coefficient is -0.21 m. These time-of-flight parameters are small and should not cause any noticeable redistribution of electrons in the longitudinal phase space unless there is an energy chirp on the electron beam with much greater amplitude than an uncorrelated energy. Nevertheless, although such a chirp is not anticipated in the FEL design now, it may be of interest for a special FEL operation in a future (as was noted by P. Emma). Fortunately, small variations in the strength of four quadrupoles between bending magnets on both sides of the lattice allows obtaining zero R56 and, therefore, to greatly reduce the sensitivity to the energy chirp. This variant of the lattice is shown in Figure 12. In order to keep this option open, we propose to use individual power supplies or correction coils for involved quadrupoles.
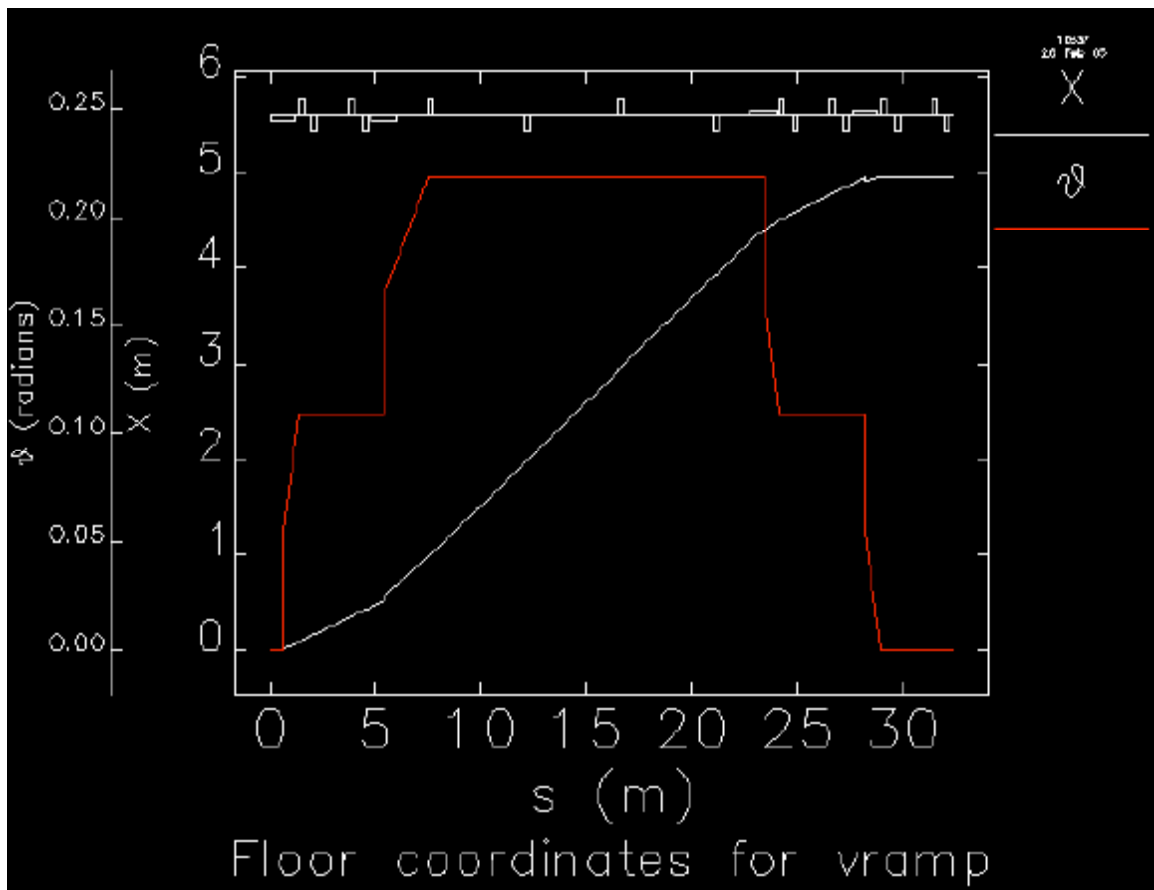


Figure 11 - The electron beam trajectory through the vertical ramp with the 12.5° ramp angle
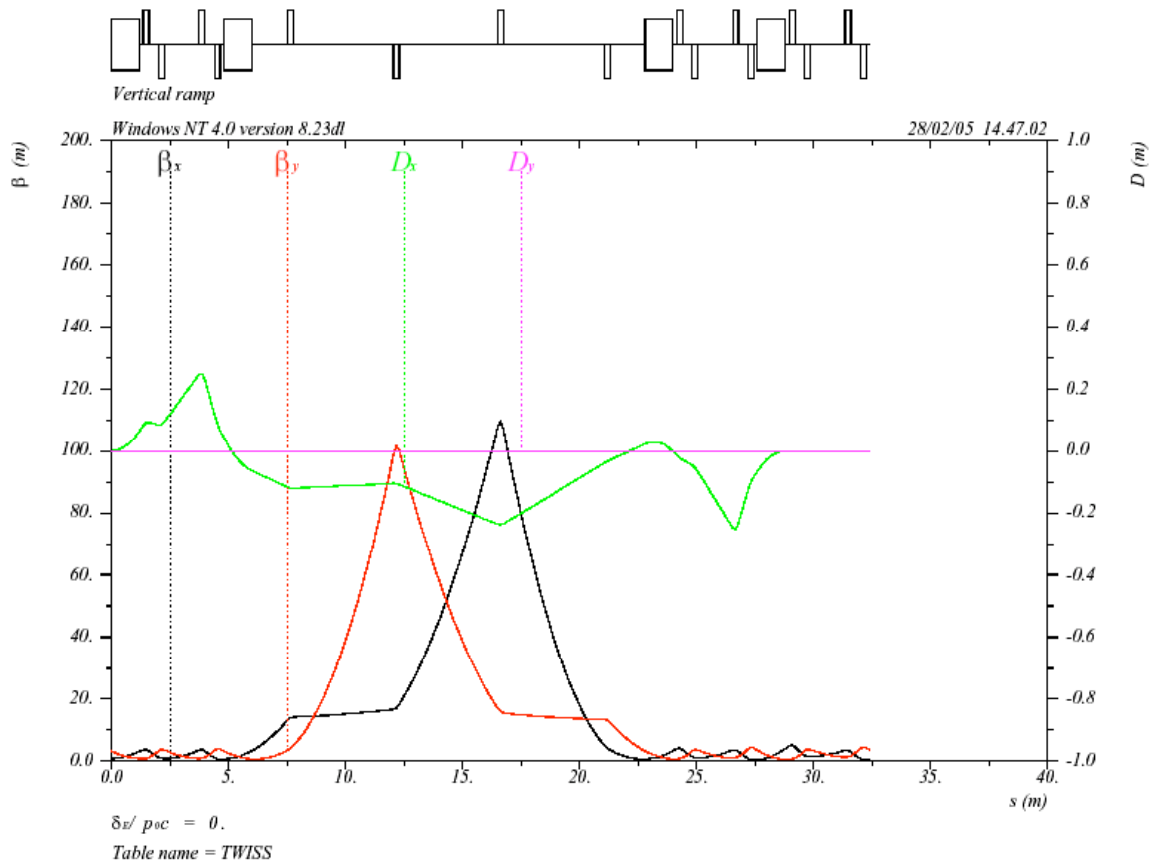
Figure 12 - The high-beta lattice modification for zero $R_{56}$

**CSR shielding by the vacuum chamber**

Coherent synchrotron radiation produced inside the vacuum chamber is weaker than free space coherent radiation assumed by the Elegant code. In order to estimate this shielding effect we followed the recipe derived in [1]. Although the analysis there was carried out for a steady state CSR wake, it should be applicable in our case as the CSR is mostly produced in the main body of bending magnets. Figure 13 shows the result obtained for the vacuum chamber with opening of 7 mm and 8 mm (the size is given for *y* direction). We show the flat-top bunch length on the horizontal axes (assuming a hard edge distribution of the peak current) and the ratio of the radiation power constrained by the vacuum chamber to a free space radiation power *PS/P0* on the vertical axes. We note that for 7 mm opening the reduction factor is approximately 50 for 1 ps bunch length and approximately 3 for 0.5 ps bunch length.

We propose to adopt a 12.5º ramp angle, allowing completion of the vertical ramp in the tunnel with the approximate length of 29 m. The lattice designed with 12.5º ramp angle shows a negligible increase in the electron beam emittance and energy spread when tested by particle tracking using the Elegant code with the following beam parameters: bunch charge of 0.5 nC, bunch length (flat top) of 1 ps, and normalized emittance of 2 mm-mrad. We also found that by increasing the charge to 1 nC and even to 2 nC, we

cause only a small and tolerable increase in the emittance. Of the two presented lattices we recommend the high-beta lattice because it presents an excellent opportunity for electron beam collimation. We recommend using individual power supplies or correction coils for all quadrupoles in order to be able to obtain zero R56. We also recommend using 7 mm gap vacuum chamber for bending magnets in order to take advantage from shielding of the CSR by the vacuum chamber. We note that the recommendation for the ramp angle was drawn independently from consideration of the shielding effect which we regard as an additional safety margin.
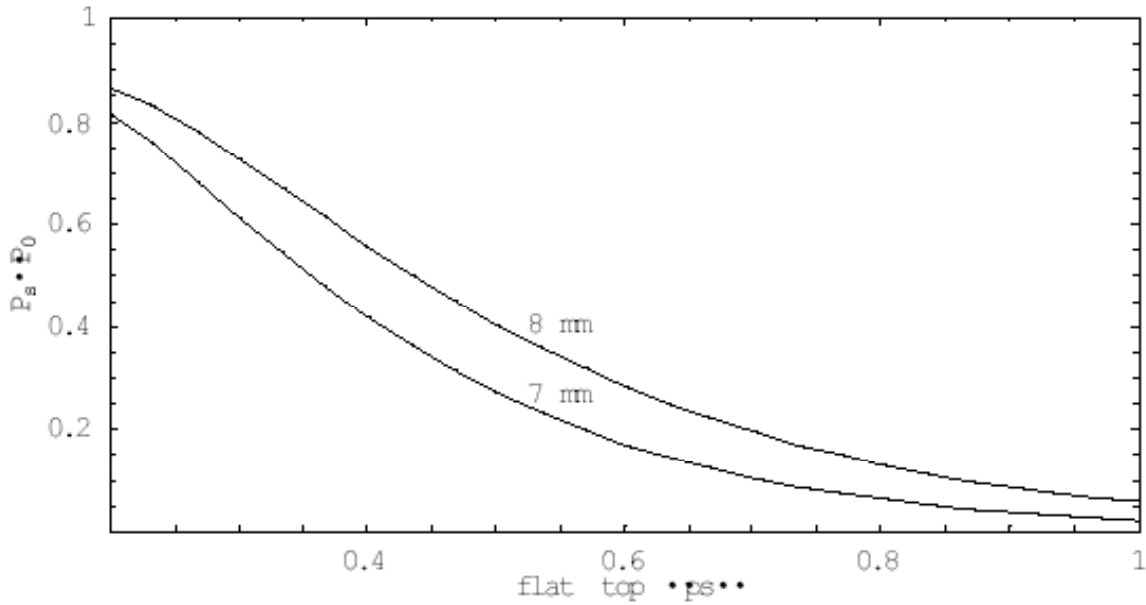


Figure 13 - Shielding effect for a vacuum chamber opening of 7 mm and 8 mm

**FEL seed laser**

We assume, we believe reasonably given existing technology, a continuously tunable laser with which to seed the electron bunch modulation in the FEL, with wavelength 240-320 nm, and with 200 MW peak power. Most of desired FEL output range, 10-105 nm, can be covered continuously by a 240-320 nm laser. Using off-the-shelf technology for rapid deployment we find 200-240 nm is available but high power is more problematic. A 320-360 nm seed laser can fill in remaining gaps up to 180 nm FEL output wavelength if desired, this will not need as much power.

Temporal coherence and tight synchronization (within 10-50 fs) of the seed laser are important requirements. We note that harmonic generation can amplify phase noise

**Undulators**

"Apple II" undulators are proposed for radiating undulators, to provide variable polarization. 52 mm and 36.6 mm period work well.

We propose longer periods for modulating undulators, and electromagnetic undulators should be considered for this application. Planar designs are suitable for modulators and for all but the final radiators, where polarization is not relevant. A large tuning range is needed, and there is a desire to simplify retuning of undulators for different wavelengths. Figure 14 shows calculated tuning range of undulators based on the Halbach formula. There is a need to study benefits of external focusing versus "natural focusing" of shaped (or helical) undulators.
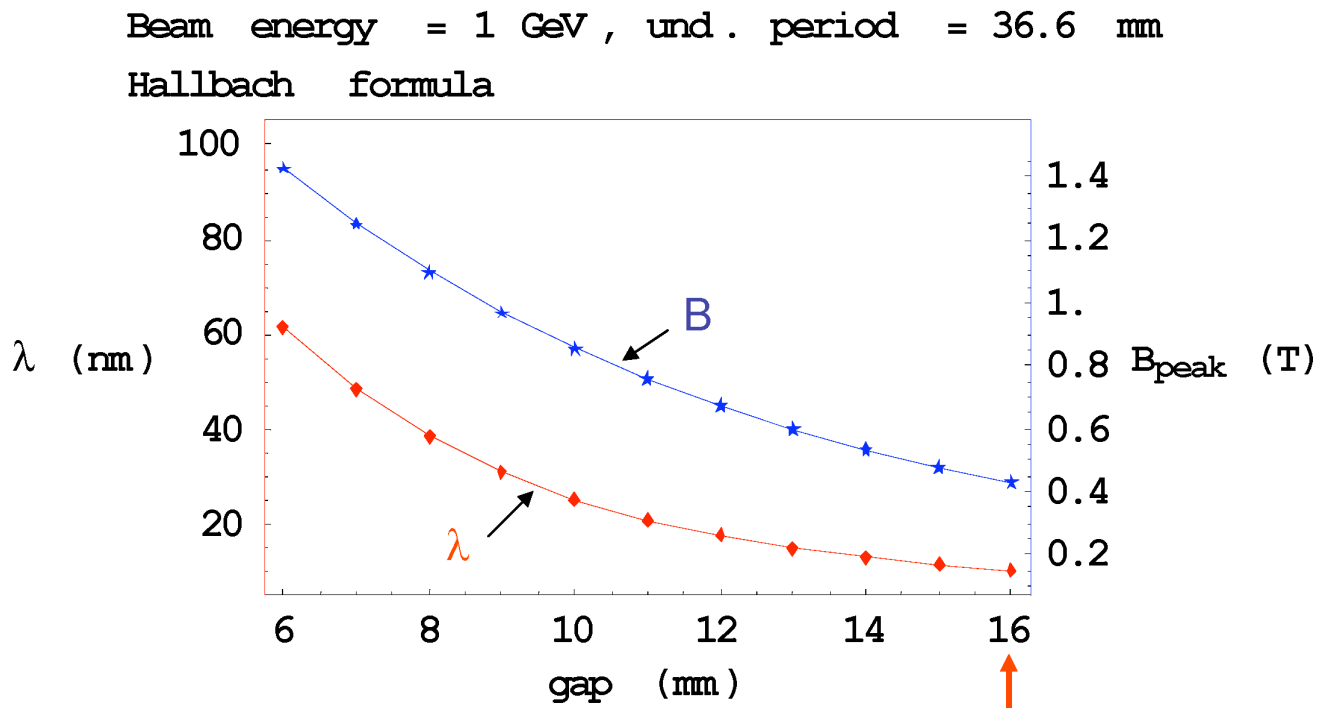


Figure 14 – Tuning range of undulators suitable to FERMI @ Elettra requirements

**Analytical studies of the seeded FEL**

The analytical FEL model developed at LBNL allows rapid calculations by suppressing FEL gain. Figure 15 shows a model harmonic cascade, Figure 16 shows the calculated FEL output dependence on wavelength and bunch compression. In this case, the electron beam energy is 700 MeV.
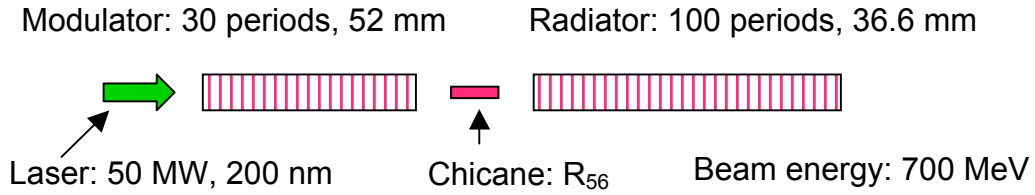
Modulator: 30 periods, 52 mm       Radiator: 100 periods, 36.6 mm

Laser: 50 MW, 200 nm       Chicane: $R_{56}$       Beam energy: 700 MeV

Figure 15 – Harmonic generation scheme

800 A, 500 keV

400 A, 250 keV
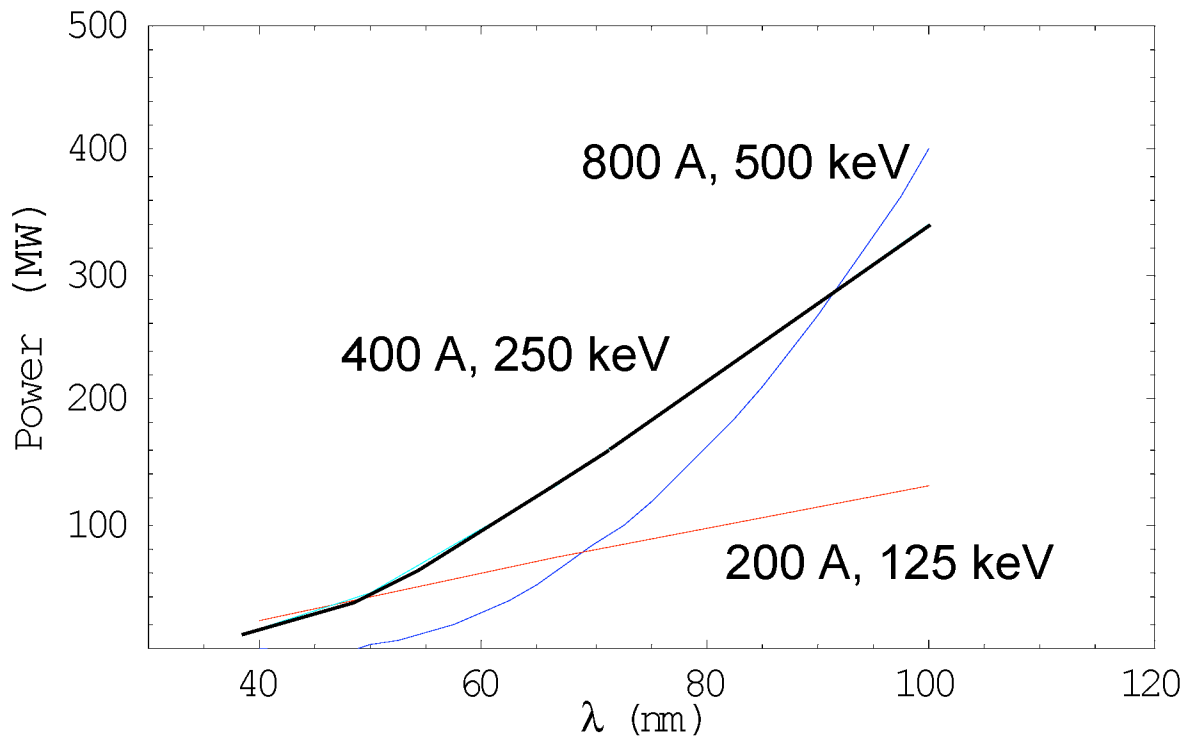
200 A, 125 keV

Power (MW)

$\lambda$ (nm)

Figure 16 – Analytical calculations of FEL output for harmonic generation scheme shown in Figure 4, for a range of electron beam peak current and energy spread

**Electron beam energy**

We have calculated performance at 700 MeV, 1 GeV, and 1.3 GeV, and as a result of this preliminary analysis we conclude that electron beam energy in excess of 700 MeV is desirable, even at 40 nm or longer FEL output wavelength.

For a 700 MeV and 1 GeV beam an undulator of 52 mm period is usable to below 40 nm.
For a 1 GeV beam, an undulator of 36.6 mm period requires rms undulator parameter $a_u \geq$ 1 down to 10 nm, and a magnet gap down to ~6 mm for 40 nm resonance.
For a 1.3 GeV beam, an undulator of 36.6 mm period requires a very small magnet gap for 40 nm resonance.

Table 3 shows parameters of various accelerator sections and the energy gain for the machine configuration of Figure 2.

Table 3 – Parameters and energy gain in accelerating sections for the configuration of Figure 2

|  | Length (m) | $P_{klystron}$ (MW) | Max./Achievable Energy Gain (MeV) | Total Energy (MeV) |
|---|---|---|---|---|
| Gun | 0.5 | 20 | 5/5 | 5 |
| S0A-B | 3.2 | 20 | 57/50 | 105 (BC1) |
| C1-3 | 4.5 | 20 | 54/54 | 263 |
| S1-4 | 6.1 | 40 (SLED) | 170/140 | 809 (BC2) |
| C4-7 | 4.5 | 20 | 54/54 | 1025 |
| S5-7 | 6.1 | 40 (SLED) | 170/140 | 1435 |

**GINGER simulations**

Table 4 shows the dependence of output power at 43 nm on peak current and energy spread using a 700 MeV energy beam, 200 MW and 300 nm laser seed, modulating undulator of 2.6 m length and 156 mm period and radiating undulator of 10.4 m length and 52 mm period.

Figure 17 shows FEL output power as a function of wavelength for the one-stage harmonic generation scheme of Figure 15.

Table 4 – GINGER calculations of 43 nm FEL output dependence on peak current and energy spread

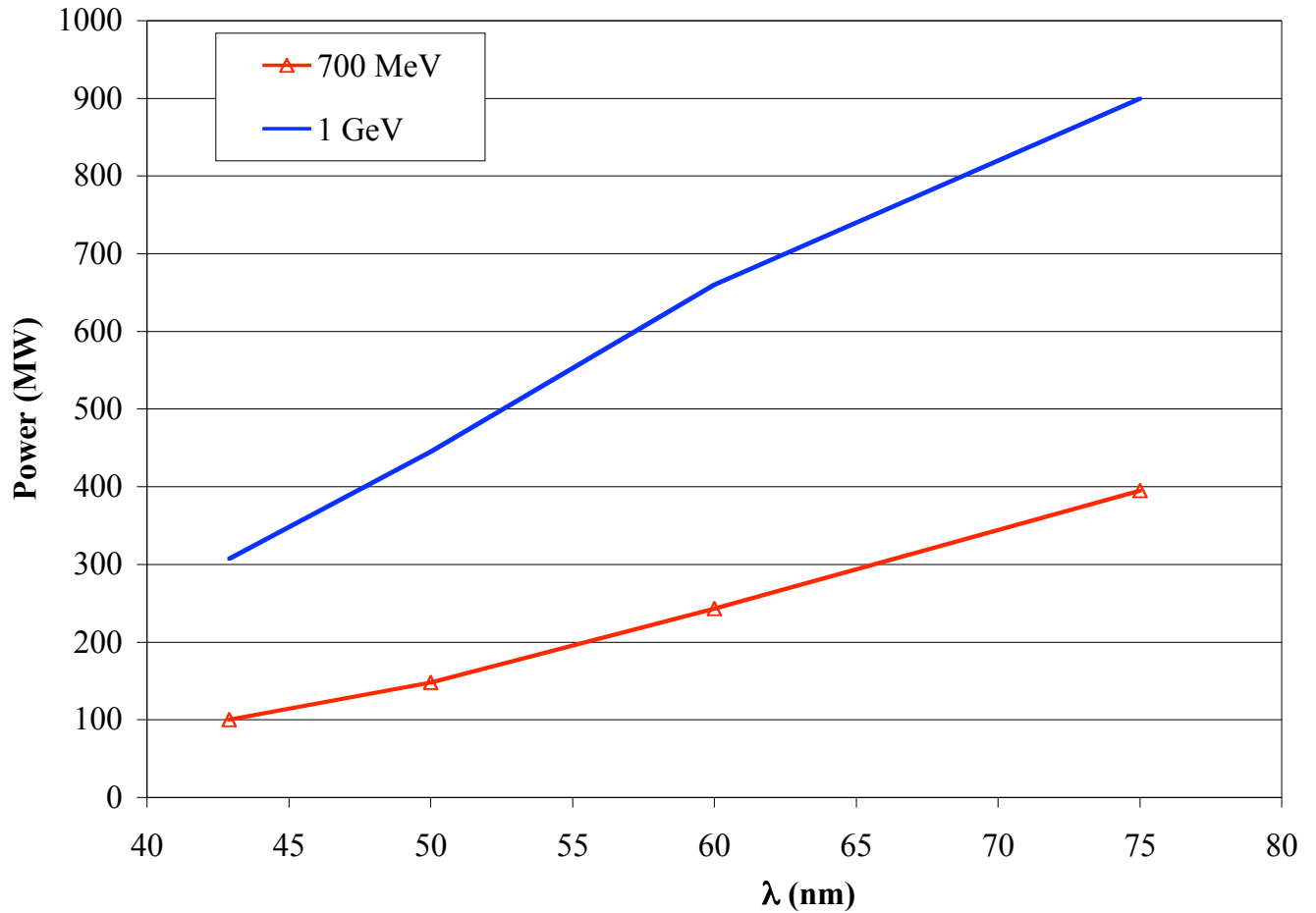| Current | Energy spread $\sigma_E$ | Power |
|---|---|---|
| 800 A | 300 keV | 152 MW |
| 400 A | 300 keV | 25 MW |
| 400 A | 150 keV | 100 MW |
| 200 A | 150 keV | 42 MW |

## Output Power vs Wavelength



Figure 17 – FEL output power as a function of wavelength for the one-stage harmonic generation scheme of Figure 4, with 400 A, 150 keV $\sigma_E$.

Figure 18 shows results of a GINGER monochromatic (time-steady) simulation using a 200 MW, 300 nm seed laser, 2.6 m modulator, 400 A beam at 1 GeV, 150 keV $\sigma_E$, e-beam matched to a $\beta=7$ m in a 43 nm FEL output wavelength radiator (7th harmonic of 300 nm). These are scatter-plots of particle gamma as a function of longitudinal phase (7 full wavelengths at 43 nm), with particles color-coded by initial phase in 300-nm modulator.
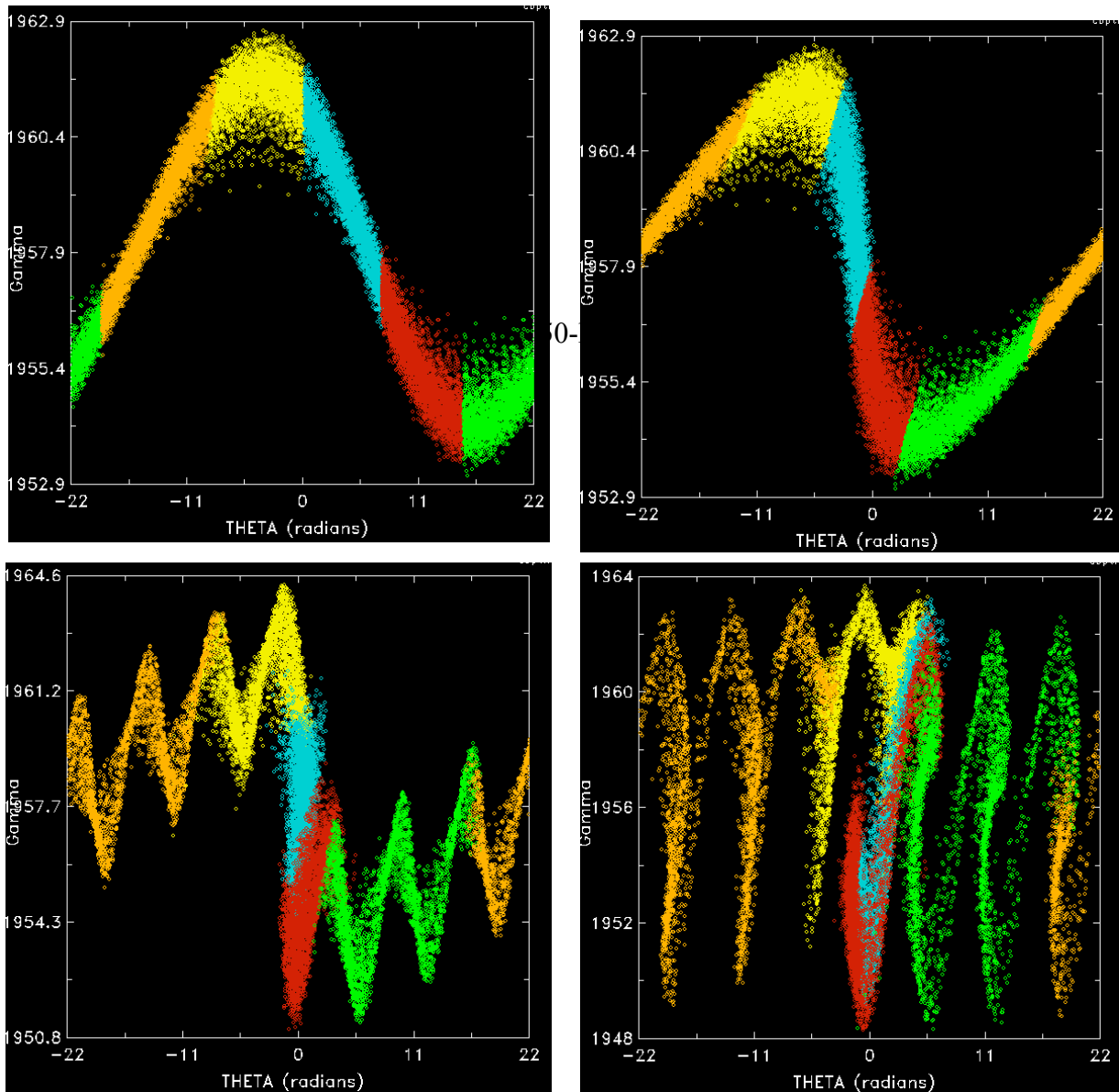


Figure 18 – GINGER steady-state simulation, scatterplots of particle energy as a function of longitudinal phase

Figure 19 shows power and bunching as a function of distance along the undulator z, for a beam of 1 GeV, 400 A, 150 keV $\sigma_E$, and for different harmonic numbers, n. In this case only undulator field strengths are adjusted.
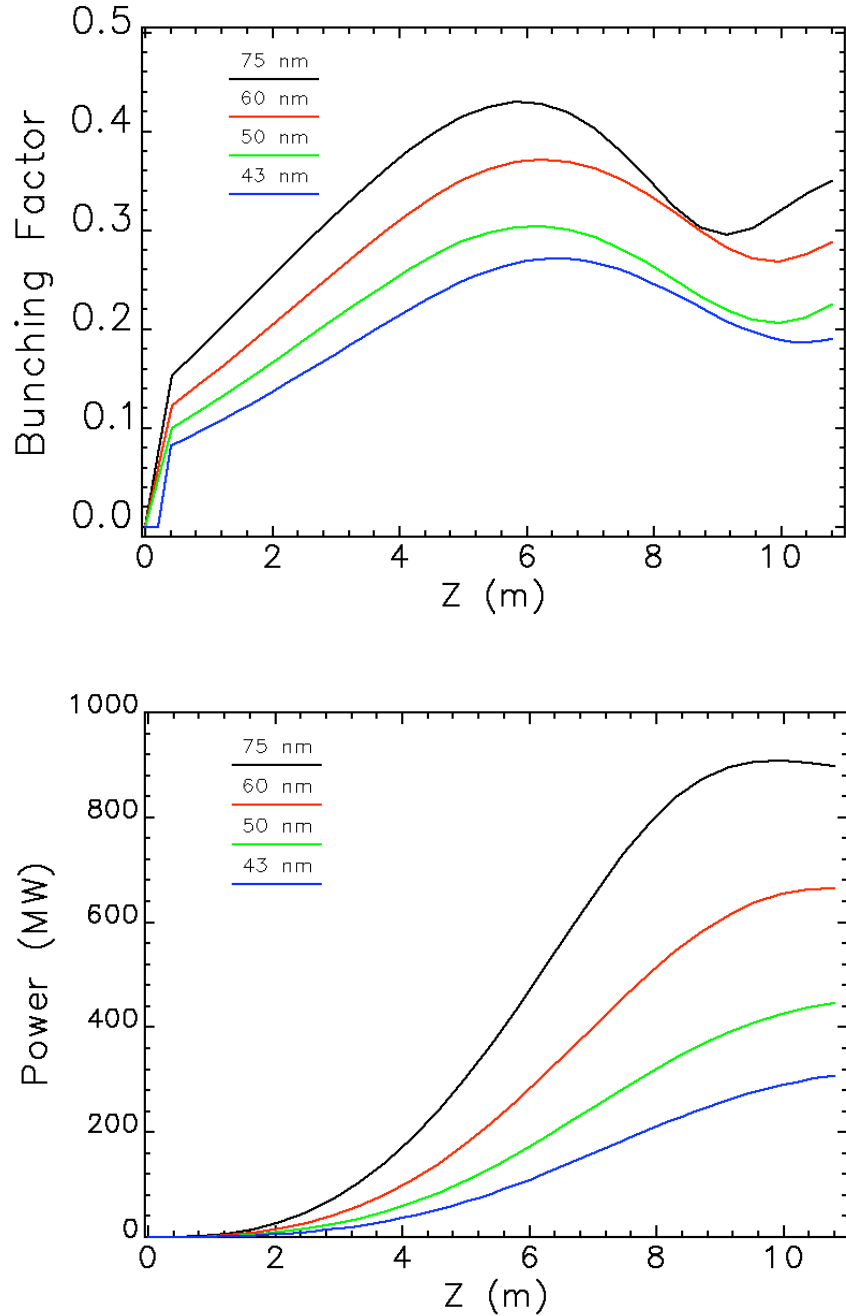


Figure 19 - Power (lower) and bunching (upper) as a function of distance z along the undulator for a 1 GeV, 400 A, 150 keV $\sigma_E$ beam, and for different harmonic numbers n.

**Two-stage simulations**

Using the GENESIS code with electron beam parameters of 1 GeV, 400 A, $\sigma_E = 150$ keV, a two-stage cascade providing 10 nm FEL output is achievable with a total length ~ 25 m. Using a 240 nm laser seed at 200 MW, the first stage converts to 40 nm in a 4.2 m undulator with 52 mm period. The final radiator is 10.2 m long with 36.6 mm period. The systems is sensitive to energy modulation, which needs to be kept below 800 keV. The first stage produces 70 MW at 40 nm, after 4.2 m, and the second stage 77 MW (at 10 nm). Figure 20 shows GENSIS calculations for this two-stage configuration.
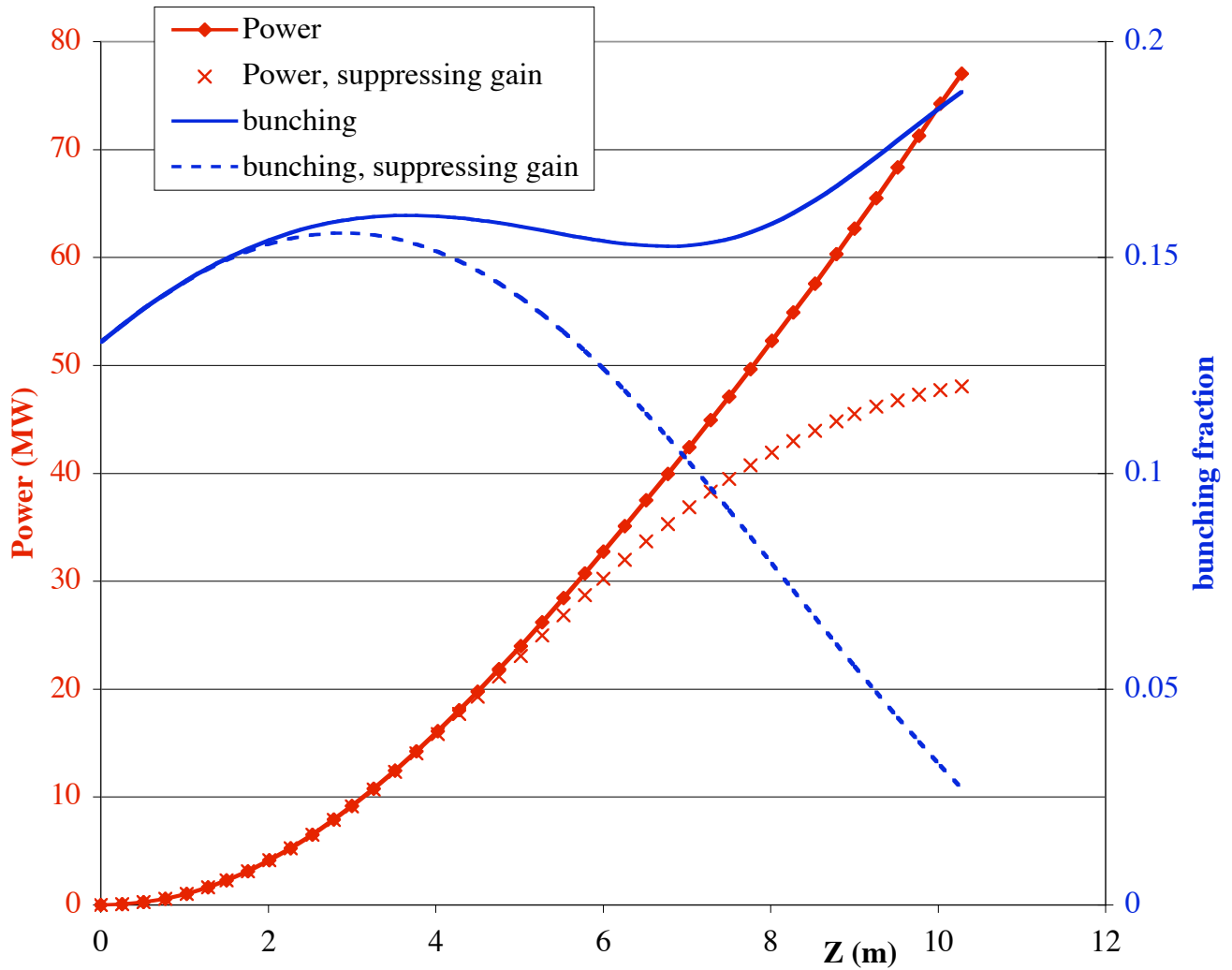


Figure 20 – GENESIS simulation results for a two-stage harmonic cascade with 10 nm output, using a 1 GeV, 400 A, 150 keV energy spread beam.

**Higher peak current through bunch compression**

Increased bunch compression provides stronger radiation output and may reduce transverse distortions arising from wakefields in the linac. There are, however, costs in terms of increase in energy spread, shorter usable pulse, and distortion from longitudinal wake field effects in the linac. The FERMI design should accommodate a range of compression ratios.

**Diagnostics requirements**

Gun exit (in a dispersive beamline)
- Energy, charge
- Spot size
- Bunch length
- Thermal emittance

Following S0A-B (100 MeV)
- Projected emittance (quad scan or slits)

Before BC1 (263 MeV) (in a dispersive beamline)
- Energy, energy spread
- Energy-time distribution (tomography)
- Slice emittance

In bunch compressors
- Centroid
- Spot size
- Collimation

In each accelerating structure
- Charge
- Centroid
- Spot size

In vertical ramp
- Centroid
- Spot size
- Collimation

**Control system**

TANGO (also used at ESRF, SOLEIL, Barcelona)

**References**

[1]     R. Li, C.L. Bohn, J.J. Bisognano, "Analysis on the steady-state coherent synchrotron radiation with strong shielding", *IEEE Proc. 1999 Part. Acc. Conf.,* 1644 (1999).